NAL TR-598T

UDC 621.45.013

TECHNICAL REPORT OF NATIONAL AEROSPACE LABORATORY

TR-598T

A Visual Observation of Cavitating Inducer Instability.

by

Kenjiro KAMIJO Takashi SHIMURA
and Mitsuo WATANABE

May. 1980

NATIONAL AEROSPACE LABORATORY

CHŌFU, TOKYO, JAPAN

A Visual Observation of Cavitating Inducer Instability.*

by

Kenjiro KAMIJO,** Takashi SHIMURA**
and Mitsuo WATANABE**

ABSTRACT

This paper presents the results of experiments on the instability of a cavitating inducer, which is considered to be closely related with the POGO phenomena in liquid propellant rockets. The present experiment employed a high speed camera for visual observations. The dynamic pressure of both the inducer upstream and downstream was also measured. The difference between rotating cavitation and cavitation induced low cycle oscillations was examined. The cavities moved around the periphery of the inducer inlet with a constant rotating speed in rotating cavitation. All cavities oscillated almost in unison in the cavitation induced low cycle oscillation. This suggests that the low cycle oscillation is a system oscillation. The high speed movie films showed the rotating cavitation process and a comparatively high rotating cavitation zone velocity. Rotating cavitation, with very low cycle cavity oscillation for each blade and steady asymmetric cavitation was also observed during the testing. In addition, the present paper illustrates the effect of inducer inlet pressure on the cavity formation.

概　　要

キャビテーティングインデューサの不安定性は液体ロケットのポゴの発生に関係しているものと考えられている。本報告はインデューサの不安定性の可視観察と圧力振動の実験結果を示したものである。主にローテーティングキャビテーションとキャビテーションに誘発された低周波振動の差異を調べた。キャビティ領域が一定の速度で旋回するローテーティングキャビテーションとは対称的に低周波振動におけるキャビティ領域はほぼ同位相で振動した。このことは低周波振動がシステム振動であることを裏づけている。キャビティ領域が低周波で振動するローテーティングキャビテーションや極端な例としての非対称キャビテーションを観察することができた。このほかインデューサ入口圧力とキャビテーションの形式を対比して示した。

1. INTRODUCTION

Cavitating inducer instability has often been encountered in liquid rocket propellant feed pumps, and according to previous works, the following four items are considered as probable causes of cavitating inducer instability.

(a) Rotating cavitation
(b) Alternate blade cavitation
(c) System oscillation
(d) Inducer inlet back flow

Rotating cavitation, which is very similar to the rotating stall in axial flow compressors, is a state in which the cavitating zones of an inducer rotates around the periphery of the inducer inlet. The appearnace and disappearance of cavitation for each blade is considered to

* Received 9 November 1979
** Kakuda Branch

produce pressure oscillations. In inducers with an even number of blades, cavitating zones seem to occur on alternate blades and, as has been reported, the cavitating zones tend to propagate from blade to blade [1][1]. If this is true, pressure oscillations may readily occur in this type of cavitation. However, alternate blade cavitation may also be considered as a kind of rotating cavitation. For instance, steady alternate blade cavitation corresponds to rotating cavitation in which an even number of cavitating zones rotates around the periphery of the inducer inlet at the same speed as the rotating blades, like steady asymmetric cavitation experienced in the present experiment of three bladed inducers. It is considered that system oscillations are caused by an interaction between inducer cavitation and pump performance, fluid circuits, etc. [2, 3, 4]. Also, it has been reported that back-flow induced prerotation could be a cause of inducer instability [5].

Cavitation induced, low cycle oscillations seem to be closely related to the POGO phenomena in liquid rockets with propellant feed pumps. However, as W.E. Young, et al. pointed out [6], it is not absolutely clear which of the above mentioned items causes the low cycle oscillations, although the cavitation induced low cycle oscillations in rocket pumps are generally believed to be a system oscillation. In system oscillations, all cavities in an inducer ought to move in unison because both inlet and discharge flowrate are expected to oscillate. To authors best knowledge there are no studies which clarify this matter.

Rotating cavitation and cavitation induced low cycle oscillations occurred in a cavitating inducer experiment in a water tunnel. The present paper describes these phenomena with reference to the difference between the two types of cavity formation.

2. APPARATUS AND PROCEDURE

2.1 Test Inducer. Two inducers utilized in this experiment had three helical and cambered blades with radial leading edges. The inducers were of the same dimensions except for the blade cant angle. The blades of one inducer (Inducer A) were not canted, while the other inducer (Inducer B) had canted blades. The blades of inducer B were perpendicular to the hub with a taper angle of 10.5 degrees. The hub ratio of the inducer inlet was 0.3 and that of the inducer outlet was 0.5. The tip solidity was 2.5. The inducers were machined from aluminum alloy. Photographs of the inducers are shown in Fig. 1 and the geometric features are listed in Table 1.

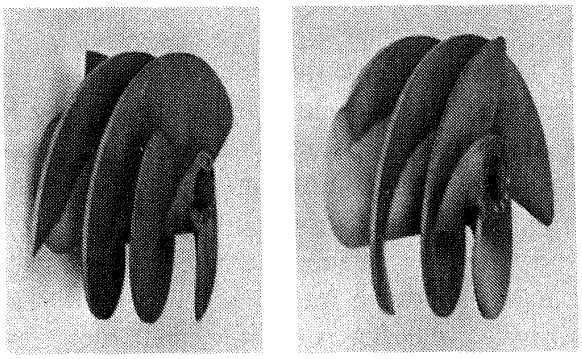

Inducer A Inducer B
(With canted blades)

Fig. 1 Inducers tested.

Tip diameter, (mm)		127.0
Inlet hub diameter, (mm)		37.0
Outlet hub diameter, (mm)		65.0
Radial tip clearance, (mm)		0.5
Number of blades		3
Solidity at tip		2.5
Blade thickness at tip, (mm)		2.5
Blade thickness at hub, (mm)		3.5
Inlet blade angle at tip, (degree)		10.0
Outlet blade angle at tip, (degree)		12.0
Hub taper angle, (degree)		21.0
Cant angle, (degree)	Inducer A	0
	Inducer B	10.5

Table 1. Constants of inducers tested

2.2 Test Facility and Test Section. This experiment was performed in a closed loop inducer test facility, a schematic diagram of which was shown in Fig. 2. The inducers were powered by a 185 KW DC motor through a multiplying gear box. The rotating speed of the motor is held constant by electrical control systems, utilizing thyristor and Ward-Leonard systems.

1. Numbers in brackets designate References at end of paper.

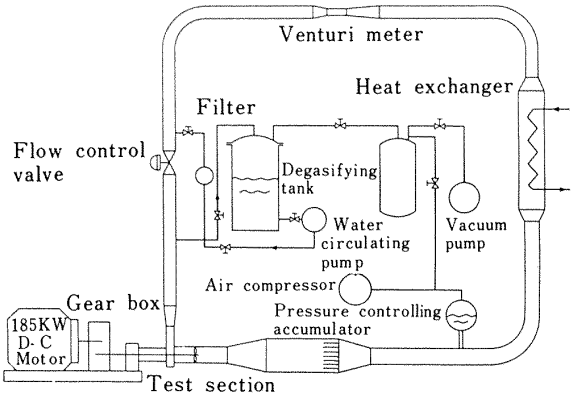

Fig. 2 Caviatation tunnel.

The facility can reduce the gas content of water to approximately 4 parts per million in weight. The gas content was measured by means of a Numachi-type apparatus [7]. The inlet pressure of the inducer was controlled by an accumulator as shown in Fig. 2. The mean flowrate was measured by means of a venturi meter. The dynamic flow rate was not measured in this experiment, but dynamic pressures were measured by means of pressure transducers, utilizing the semi-conductor piezo resistance effect. The pressure transducers were installed in the inducer casing approximately 65 mm upstream and 12 mm downstream of the leading and trailing edges for inducer A and 57 mm and 18 mm for inducer B. The dynamic pressures measured by the transducers were recorded on an FM data recorder made by Ampex Corporation. The test section is shown in Fig. 3. The inducer casing was made from transparent plastic to permit visual observations. The shaft speed was measured by a magnetic pulse pick-up.

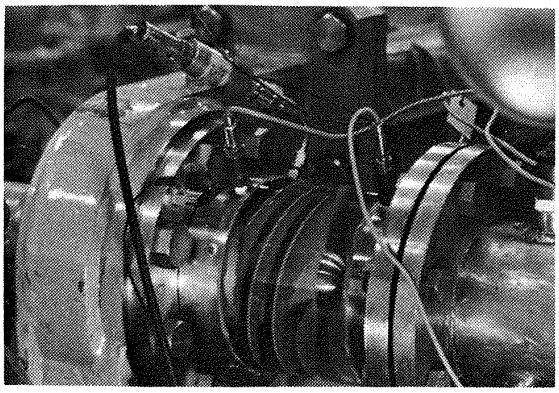

Fig. 3 Inducer test section.

2.3 Procedure. Water was degasified before every test until the air content was less than 4 parts per million by weight. The water temperature was held constant using a heat exchanger during all operations. Data was taken in groups of constant shaft speed and constant flowrate, while inducer inlet pressure was varied from high to low and vice versa. Photographs were first taken using 16 mm film at 18 frames per second. The stroboscopic light was triggered by the magnetic pulse pick-up on the shaft so that the motion of the inducer appears to stop and the same blade can be observed. High speed movie pictures were taken, using a continuous light source, at a framing rate of from 2,500 to 8,000 frames per second. A view of test section with high speed camera and light sources is shown in Fig. 4.

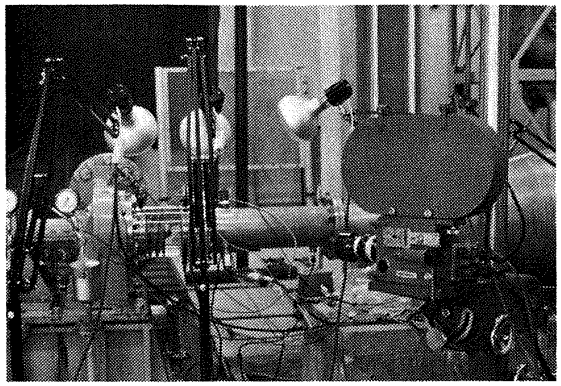

Fig. 4 View of test section with high speed camera and light sources.

3. EXPERIMENTAL RESULTS AND DISCUSSION

3.1 Suction performance of Test Inducers. Fig. 5 shows the suction Performance of the test inducers relevant to the following discussion on cavitating inducer instability. These results were obtained in groups of constant shaft speed and constant flowrate, while the inducer inlet pressure was varied. At higher cavitation number the two inducers showed almost identical head coefficients. Moreover, the difference in suction performance between the two inducers was very small. With respect to steady state characteristics, the two inducers exhibited almost identical performance regardless of canted or uncanted blades. However, inducer B (with canted blades) caused more severe inlet pressure fluctuations and operation created much more noise than inducer A, as mentioned later.

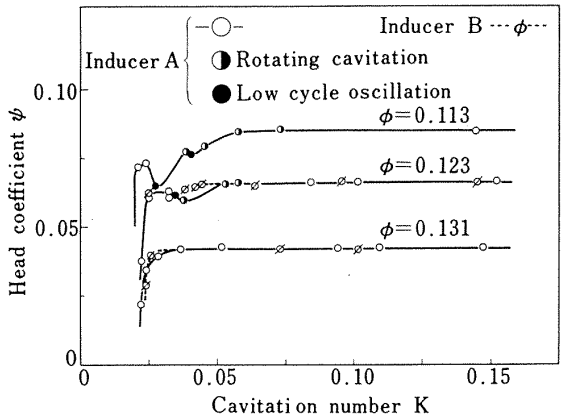

Fig. 5 Suction performance of test inducers.

3.2 Rotating Cavitation. The test inducers exhibited rotating cavitation with severe pressure fluctuations. The rotating cavitation occurred within specific regions of inducer inlet pressure for constant shaft speed and constant flowrate. The regions, as shown in Fig. 5, are only for inducer A (without canted blades). Rotating cavitation occurred even at comparatively high cavitation number. High speed movie pictures of the rotating cavitation are shown in Fig. 6-a and 6-b. One series of the pictures shown in Fig. 6-a presents one cycle cavity oscillations on one blade of inducer A. Another series shown in Fig. 6-b presents the cavity variation on three blades in a 2/3 revolution of the shaft. Fig. 7 presents the variation of the approximate cavity length with time. This figure shows both the tip vortex and blade surface cavity length. The cavity length was measured from high speed movie films. Although this method probably brought about some error, because of the obscurity of the end of cavities, particularly in the case of blade surface cavitation, it gave us useful information,

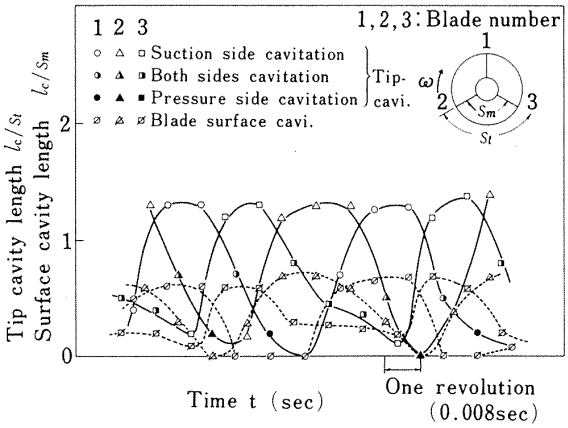

Fig. 7 Fluctuations of cavity length in rotating cavitation.

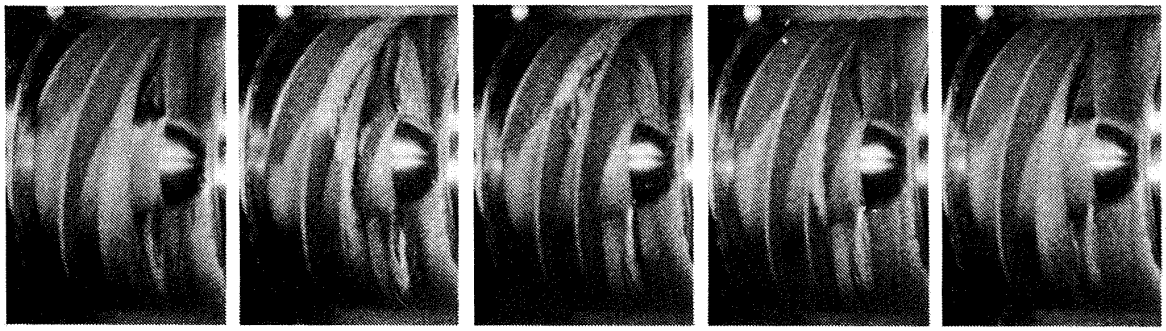

N=7,500RPM, K=0.045, ϕ=0.094

Fig. 6-a Sequence of cavity fluctuation on one blade in rotating cavitation.

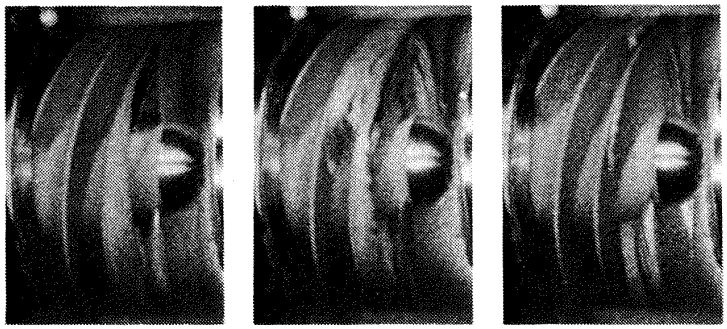

Blade number 1 Blade number 2 Blade number 3

N=7.500RPM, K=0.045, ϕ=0.094

Fig. 6-b Sequence of cavity fluctuation on three blades.
(Three pictures correspond to 2/3 revolutions of a shaft.)

like in Fig. 7, for use in the following discussions. All rotating cavitation observed in the present experiments showed almost the same characteristics as that shown in Fig. 7. The blade surface cavity length was measured at the middle of the blade height. The length of the tip vortex cavitation was measured along the tip of the blades. The high speed movie films showed that the cavities on the blade surface near the tip fluctuated more severely than at the middle of the blade height. It is interesting to note that both the tip and blade surface cavities on one blade oscillate with almost the same frequency and phase. It should be noted that Fig. 7 shows only cavity length variations and does not show cavity volume variations. However, there may be some relationship between the cavity length and cavity volume. Fig. 7 clearly shows that both the tip vortex and blade surface cavitation rotate around the periphery of the inducer inlet at a constant rotating speed. Another point worthy of mention is that the angular velocity of the rotating cavitation, ω_S, is slightly higher than that of the blades, ω, according to Fig. 7. In other words, the rotating direction of the cavitating zones against the rotating blades is the same as that of the shaft. This characteristic differs greatly from that of the rotating stall experienced in axial flow compressors. However, we must consider the number of cavitating zones in the inducer, in order to discuss the rotating velocity in more detail. In rotating cavitation, it might be possible to assume the following expression of cavity length, $\ell_c(t)$.

$$\ell_c(t) = \ell_c \sin(n\theta - \omega_S t) \qquad (1)$$

The variation in cavity length of the rotating cavitation demonstrated in Figs. 6-a, 6-b and 7, measured against one point of the casing wall, is shown in Fig. 8. The cavity length data were presented intermittently due to the small number of blades. The solid line in Fig. 8 shows the cavity length variation expressed in equation (1). The variation in cavity length against another point, an arbitrary angle apart from the former point, was easily determined using Fig. 7. This is shown by the dotted line in Fig. 8. The following expressions can also be employed in rotating cavitation.

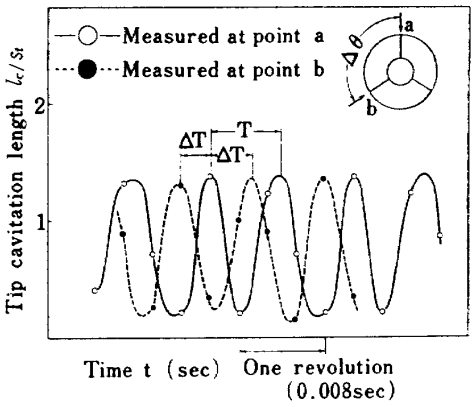

Fig. 8 Fluctuation of cavity length in rotating cavitation.

$$n = \frac{2\pi \cdot \Delta T}{\Delta\theta \cdot T} \qquad (2)$$

$$\omega_S = \frac{2\pi}{n \cdot T} \qquad (3)$$

Assuming that the rotating velocity of the cavitating zones is higher than that of blades, ΔT and T are about 0.0023 and 0.0068 seconds, respectively, when $\Delta\theta$ is $(2/3)\pi$ according to Fig. 8. Thus the number of the cavitating zones, n, is one and we get $\omega_S = 1.16\omega$. However, we can also assume that the rotating velocity is lower than that of the blades. In this case ΔT and T are 0.0047 and 0.0068 seconds respectively, and we get $n = 2$ and $\omega_S = 0.59\omega$. Therefore, we cannot determined uniquely the rotating velocity of the rotating cavitation. It is more probable that one cavitating zone exists in a three bladed inducer. Further, steady asymmetric cavitation, which will be mentioned later, can be considered to be a rotating cavitation of $\omega_S = \omega$ and $n = 1$. Therefore, a possibility of the higher rotating velocity than that of blades might be totally undeniable from the present experiment.

The variation in tip vortex cavitation in Fig. 7 exhibits a kind of circumferentially non-uniform flow. It is well known, that a larger angle of attack of an inducer inlet, causes more severe tip vortex cavitation and makes blade surface cavity thicker. According to this fact, we know that a larger angle of attack occurs in one leading edge spacing and a smaller or negative angle of attack in other spacings from Fig. 7. In Fig. 7 suction side cavitation, pressure side cavitation and both side cavitation are distinguished. It

can also be seen in the series of pictures in Fig. 6-a, which show one cycle cavity oscillation on one blade. The rotating cavitation shown in Figs. 6-a, 6-b and 7 is schematically presented in Fig. 9.

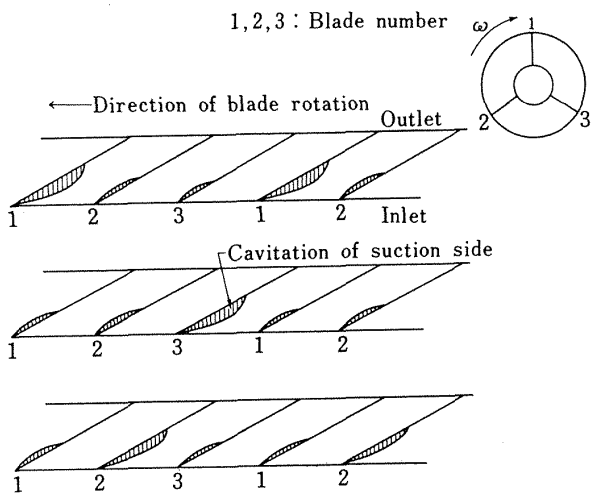

Fig. 9 Depiction of rotating cavitation pattern.

Pressure fluctuations measured upstream and downstream of inducer A are shown in Fig. 10, which corresponds to the rotating cavitation mentioned above. Severe pressure oscillations of approximately 60 Hz appeared at the inducer upstream, while the downstream pressure showed little corresponding oscillations. This fact suggests that rotating cavitation is only associated with inlet flow conditions and does not cause mean flow rate variations at the inducer upstream and downstream, which could have been easily assumed by equation (1). The frequency of cavity length oscillation in Fig. 7

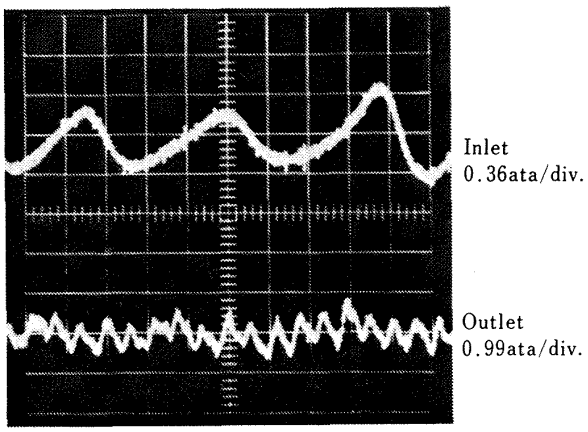

N=7,500RPM, K=0.045, ϕ=0.094

Fig. 10 Pressure oscillations in rotating cavitation.

coincides with that of pressure oscillations in Fig. 10. However, the relationship was too complicated to state that in general cavity and pressure oscillations do coincide in frequency.

Clearer high speed pictures of rotating cavitation are shown in Fig. 11, which corresponds to Fig. 12. This rotating cavitation showed almost the same characteristics as that shown in Figs. 6-a and 6-b, as mentioned before.

In the rotating cavitation we found that the frequency of cavity length oscillations tended to decrease along with a decrease in inducer inlet pressure. For instance, about 1 Hz cavity oscillation on one blade appeared. Further, it should be noted that the cavity length fluctuations almost stopped and steady asymmetric cavitation appeared in an extreme case. The high speed pictures of this cavitation are shown Fig. 13. In this particular cavitation, three different steady cavity shapes occurred on three blades. These cavitating zones rotated around the periphery of the inducer inlet at the same speed as the rotating blades. This cavitation is considered to be a kind of rotating cavitation and corresponds to steady alternate blade cavitation, that appears in an inducer with an even number of blades. The upstream pressure of the steady asymmetric cavitation is shown in Fig. 14. The frequency of the pressure oscillations in Fig. 14 coincides with the shaft rotative speed. This fact makes it clear that the number of cavitating zones of the steady asymmetric cavitation shown in Fig. 13 is one, that is n = 1.

The relationship between cavity oscillation frequency and cavitation number and flow coefficient, which was obtained from high speed movie films, is shown in Fig. 15. The decrease of cavitation number and flow coefficient brings about the decrease of cavity oscillation frequency. It is well known that the decrease of cavitation number and flow coefficient increases cavity volume of an inducer. This increase of cavity volume is considered to decrease cavity oscillation frequency.

3.3 Cavitation Induced Low Cycle Oscillation. Cavitation induced low cycle oscillations also occurred in the same experiment described in the previous section. These oscillations differed greatly from the rotating cavitation with

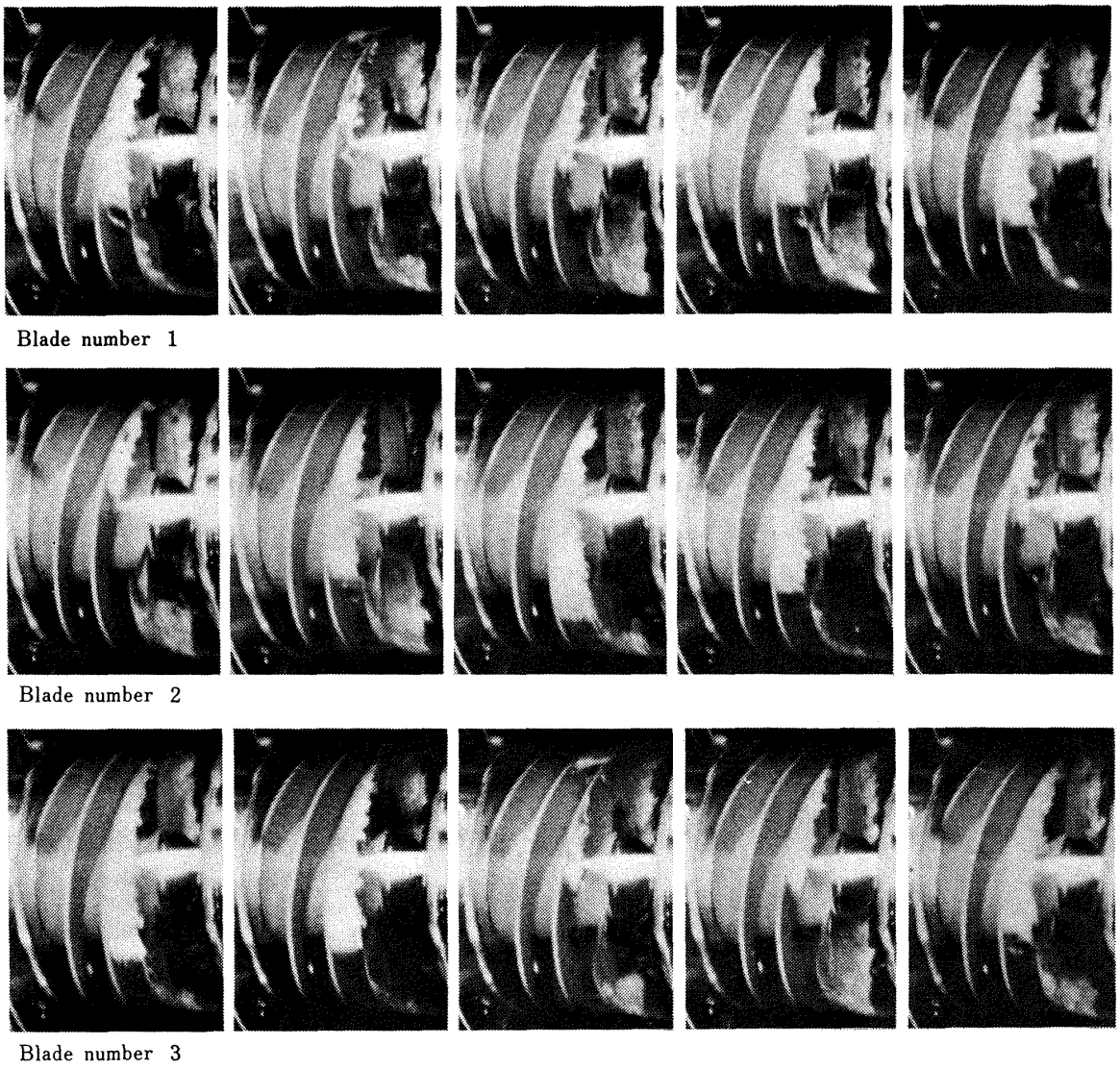

Fig. 11 Sequence of cavity fluctuation on three blades in rotating cavitation.

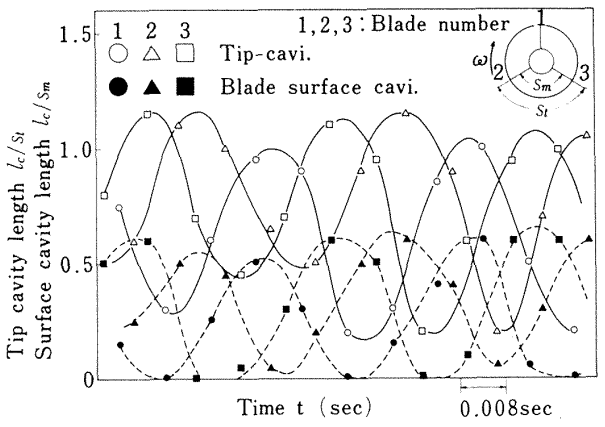

Fig. 12 Fluctuation of cavity length in rotating cavitation.

low cycle cavity oscillations. The regions in which the cavitation induced low cycle oscillations appeared, are shown in Fig. 5. It is interesting to note that the low cycle oscillations occurred within the regions where the slope of the suction performance curve in Fig. 5 was negative. The oscillations tended to be more severe at a lower flowrate. High speed movie pictures of the low cycle oscillations of inducer A are shown in Fig. 16. One series shows cavitation at a lower inlet pressure of one cycle of pressure oscillations and the other series' cavitation at a higher inlet pressure. Each series is composed of three pictures which correspond to a 2/3 revolution of the shaft. Fig. 17 shows the relationship between the approximate cavity length and time. These low cycle oscillations differ noticeably from the rotating

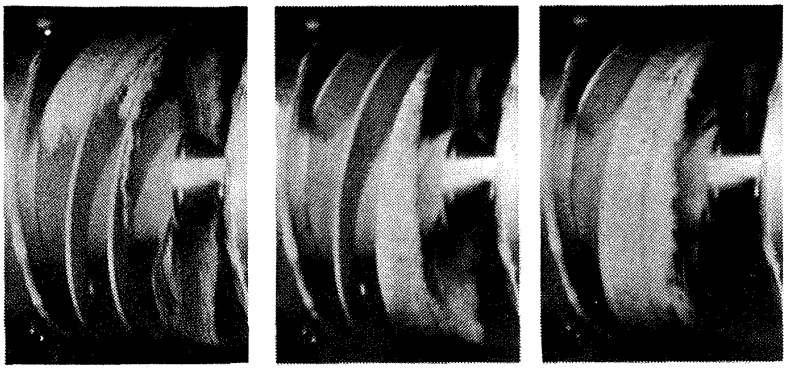

Blade number 1 Blade number 2 Blade number 3

N=7,500rpm, K=0.037, ϕ=0.118

Fig. 13 Steady asymmetric cavitation.

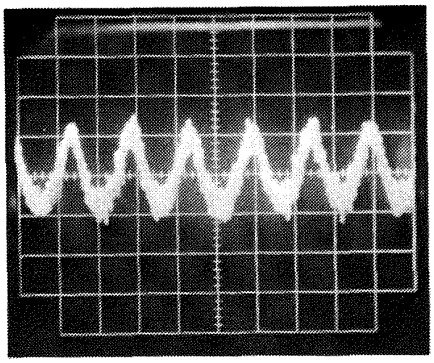

0.338ata/div.

50ms/div.

$f_p \fallingdotseq 125Hz$

Fig. 14 Upstream pressure oscillations in steady asymmetric cavitation.

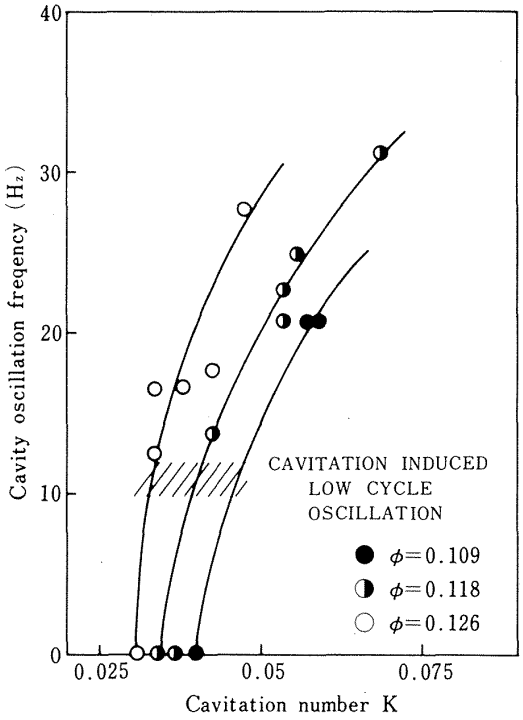

Fig. 15 Cavity oscillation frequency of rotating cavitation.

cavitation as shown in Figs. 6-a, 6-b and 11, in that the cavities of all blades oscillate in near unison. In other words, all cavities oscillate with almost the same frequency and phase. This difference has not been made clear, although the low cycle oscillations often experienced in rocket pumps are generally believed to be system oscillations in which the cavities must oscillate in unison.

The upstream and downstream pressures of the low cycle oscillations are shown in Fig. 18. The downstream pressure oscillates severely at the same frequency as the upstream pressure in contrast to the pressure fluctuations in Fig. 10. In this low cycle oscillation, the cavities and pressure oscillate at the same frequency as that shown in Figs. 17 and 18.

The two facts, that the cavities oscillated almost in unison and that the downstream pressure exhibited corresponding oscillations to the upstream pressure, suggest that the mean flowrate oscillations occurred in both inducer upstream and downstream. Further, the oscillations appeared within the regions where the slope of the suction performance curve was negative. From these facts it can be concluded that the cavitation induced low cycle oscillations experienced in the present experiments are a cavitation induced system oscillation.

The wave of upstream pressure fluctuations shown in Fig. 18, is very complex and differs from that of the rotating cavitation shown in

Fig. 10. In Fig. 17 a slight trend of rotating cavitation appeared in the region where the cavity length becomes minimum. The complex shape of the upstream pressure wave may be due to this added feature.

With regard to the relationship between inducer inlet backflow and cavitation induced low cycle oscillations, the oscillations occurred in spite of a very small backflow as shown in Fig. 16. However, the low cycle oscillations tended to be more severe at a lower flowrate; thus it is possible that backflow is related to

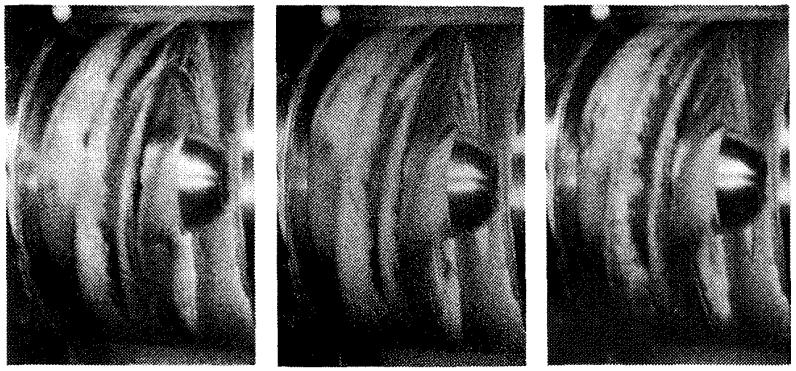

Blade number 1 Blade number 2 Blade number 3

Lower inlet pressure

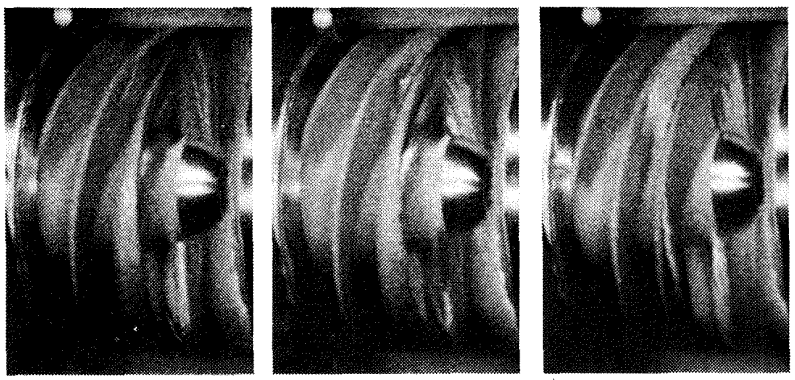

Higher inlet pressure

N=7,500RPM, K=0.026, ϕ=0.104

Fig. 16 Sequence of cavity fluctuation on three blades in low cycle oscillation. (Each three pictures correspond to 2/3 revolutions of a shaft.)

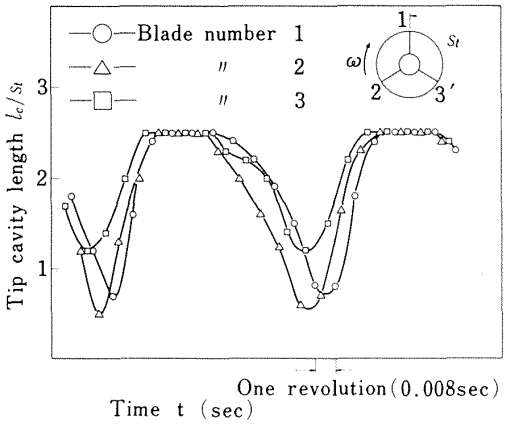

Fig. 17 Fluctuation of cavity length in cavitation induced low cycle oscillation.

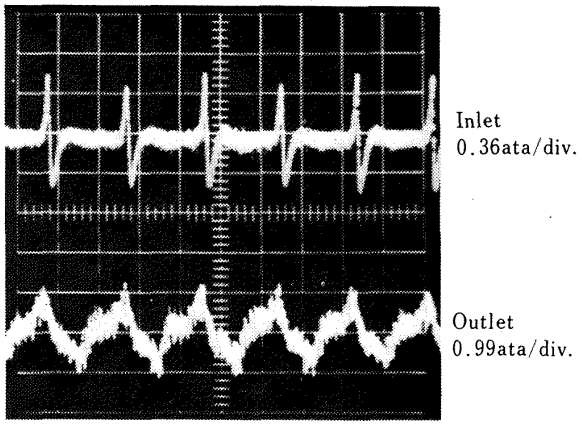

N=7,500RPM, K=0.026, ϕ=0.104

Fig. 18 Pressure oscillation in cavitation induced low cycle oscillation.

this kind of oscillation.

3.4 Pressure Fluctuation and Types of Cavitation. We would like to describe the relationship between suction pressure, upstream and downstream pressure fluctuations and types of cavitation in more detail. Fig. 19 shows typical upstream and downstream pressure fluctuations of inducer A. Rotating cavitation appears at a comparatively high suction pressure, as shown in Figs. 19-c and 19-d. With the decrease in the inlet pressure, there also appears a lower inlet pressure fluctuation frequency. A further decrease in inlet pressure causes cavitation induced low cycle oscillation or a combination of low cycle oscillation and rotating cavitation as shown in Fig. 19-e. A slight additional decrease in inlet pressure, however, causes a steady asymmetric cavitation to appear. Here again, a slight additional decrease in inlet pressure causes low cycle oscillations with the cavity oscillation in unison. Finally steady fully developed cavitation appears as shown in Fig. 19-h.

Inducer B (with canted blades) operation was much noisier than inducer A, and exhibited rotating cavitation with very severe upstream pressure oscillations. The upstream and downstream pressure fluctuations are shown in Fig. 20. The downstream pressure showed a small oscillation corresponding to the upstream pressure. This was probably due to too severe upstream pressure oscillations.

4. CONCLUDING REMARKS

Rotating cavitation and cavitation induced low cycle oscillations occurred in a cavitating inducer experiment in a water tunnel. Utilizing high speed movie films, photographs from 16mm films and dynamic pressure measurements at inducer upstream and downstream,

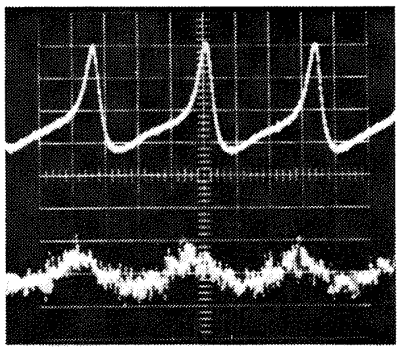

5 ms/div.

N=7,500 RPM, K=0.055, ϕ=0.122

Fig. 20 Pressure oscillation in rotating cavitation of inducer B.

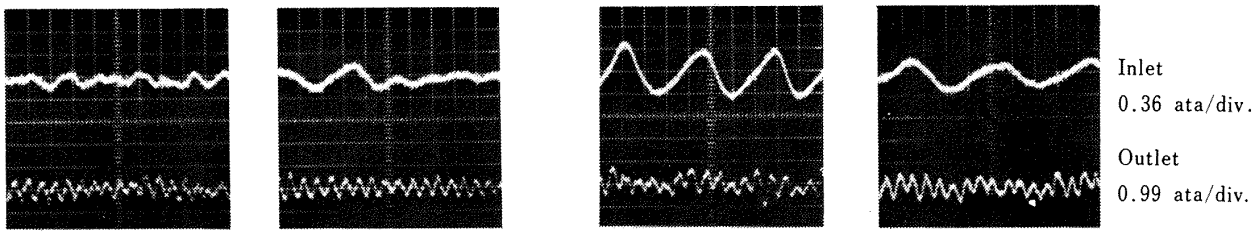

K=0.144, 5 ms/div. (a) Steady symmetric cavitation

K=0.073, 5 ms/div. (b) Combination of steady symmetric and rotating cavitation

K=0.057, 5 ms/div. (c) Rotating cavitation

K=0.045, 5 ms/div. (d) Rotating cavitation

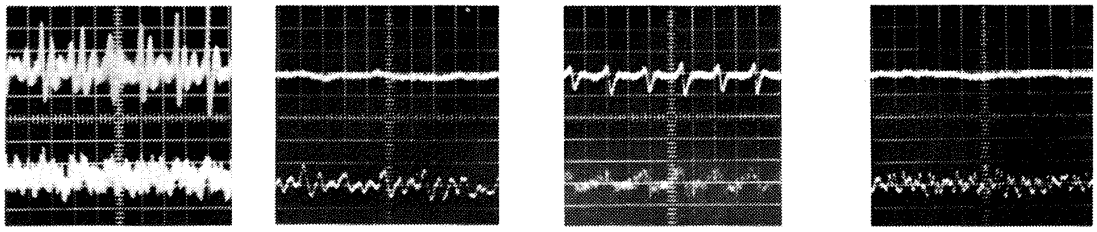

K=0.040, 50ms/div. (e) Combination of rotating cavitation and low cycle oscillation

K=0.038, 50ms/div. (f) Steady asymmetric cavitation

K=0.027, 50ms/div. (g) Low cycle oscillation

K=0.024, 5 ms/div. (h) Fully developed cavitation

Fig. 19 Relation between suction pressure and pressure fluctuation.

the authors have examined these two types of cavitation. The difference between rotating cavitation and cavitation induced low cycle oscillations in the present experiment is as follows:

- Upstream pressure oscillations in rotating cavitation are more severe than the downstream pressure oscillations.
- In cavitation induced low cycle oscillations, serious pressure oscillations occurred in both upstream and downstream pressure.
- Cavities of three blades oscillated almost in unison in the cavitation induced low cycle oscillations.

Judging from these facts and the fact that the cavitation induced low cycle oscillations occurred when a suction performance curve had a negative slope, it is considered that the low cycle oscillations are system oscillations.

With regard to rotating cavitation, the high speed movie films showed the rotating cavitation process and a comparatively high rotating cavitation zone velocity. In rotating cavitation, very low frequency cavity oscillations appeared and steady asymmetric cavitation occurred in extreme cases. This asymmetric cavitation can be considered to correspond to steady alternate blade cavitation of an inducer with an even number of blades. The high speed movie films also show that circumferentially non-uniform flow at the inducer inlet was closely related to rotating cavitation.

In this experiment the relationship between pressure oscillations and cavity oscillations in rotating cavitation could not be made completely clear. Moreover, the transition from rotating cavitation to cavitation induced low cycle oscillations was too complicated to be explained in detail.

ACKNOWLEDGMENT

The authors would like to express their gratitude to Mr. T. Ohtsuka, a director of Kakuda Branch of National Aerospace Laboratory, for his generous advice. The authors also would like to express their gratitude to Dr. A.J. Acosta and Dr. C. Brennen in California Institute of Technology, for their interest and valuable suggestions and advice.

NOMENCLATURE

K	:	Cavitation number, $(p_i-p_c)/(\rho w_i^2/2)$
$\ell_c(t)$	:	Instantaneous cavity length
ℓ_c	:	Cavity length
N	:	Inducer rotating speed
n	:	Number of cavitating zones
ΔH	:	Inducer static head obtained from inducer upstream and downstream casing wall static pressures.
P_i	:	Inducer inlet static pressure
P_c	:	Vapour pressure
s_t	:	Solidity at tip
s_m	:	Solidity at middle of blade height
T	:	Period (See Fig. 8)
ΔT	:	Time delay (See Fig. 8)
t	:	time
u_t	:	Inducer inlet tip rotating velocity
v_i	:	Inducer inlet mean axial fluid velocity
w_i	:	Inducer inlet relative fluid velocity
ϕ	:	Flow coefficient, v_i/u_t
ψ	:	Head coefficient, $\Delta H/(u_t^2/g)$
ρ	:	Density
θ	:	Angle
$\Delta\theta$	:	Angle between two points (See Fig. 8)
ω	:	Angular velocity of blades
ω_s	:	Angular velocity of rotating cavitation

REFERENCE

1. Acosta, A.J., "An Experimental Study of Cavitating Inducer", Proceeding of the Second Symposium on Naval Hydrodynamic, ONR/ACR-38, 1958, pp.537-557.
2. Sack, L.E. and Nottage, H.B., "System

Oscillations Associated With Cavitating Inducer", Journal of Basic Engineering, Trans. ASME Series D, Vol. 87, 1965.
3. Brennen, C. and Acosta, A.J., "The Dynamic Transfer Function for a Cavitating Inducer", Journal of Fluid Engineering. Trans. ASME, Series I, Vol. 98, 1976, pp.182-191.
4. Ng, S.L., "Dynamic Response of Cavitating Turbomachines", Ph. D. Thesis, California Institute of Technology, Dept. of Mechanical Engineering, 1976.
5. Badowski, H.R., "An Explanation for Instability in Cavitating Inducer", ASME 1969 Cavitation Forum.
6. Young, W.E., et al, "Study of Cavitating Inducer Instabilities", NASA CR-123939, 1972.
7. Numachi, F., et al, "Study on Mechanism of Cavitation Inception", Trans. JSME, Vol. 3, 1973, pp.177-182.

TECHNICAL REPORT OF NATIONAL
AEROSPACE LABORATORY
TR-598T

航空宇宙技術研究所報告 598T 号(欧文)

昭和55年5月発行

発行所　航空宇宙技術研究所
東京都調布市深大寺町1,880
電話 武蔵野三鷹(0422)47-5911(大代表)
印刷所　株式会社　三興印刷
東京都新宿区信濃町12

Published by
NATIONAL AEROSPACE LABORATORY
1,880 Jindaiji, Chōfu, Tokyo
JAPAN